

Chapter 9

Emissions of PM_{2.5}-Bound Trace Metals from On-Road Vehicles: An Assessment of Potential Health Risk



Jai Prakash and Gazala Habib

Abstract The present study elucidates on PM_{2.5} (particle aerodynamic diameter $\leq 2.5 \mu\text{m}$) bound trace metals characterization from on-road light-duty vehicles during on-road operation and their health risk assessment for adults and children. The vehicles assessed in present work included 4-wheelers passenger cars with a different age group of Bharat Stage (BS) II, III, and IV and different fuel type [diesel, gasoline and compressed natural gas (CNG)]. To understand the particle losses, particle formation, and homogenous mixing, firstly, a new portable dilution system (PDS) was designed for diluting the exhaust with adequate aerosol formation and growth, and evaluated beforehand under controlled condition in laboratory for diesel vehicles over a wide range of dilution ratio (30:1, 60:1, and 90:1). For on-road experiments, a PDS, a heated duct, a gas analyzer, an exhaust velocity probe, a temperature, and relative humidity probe were mounted on Aerosol Emissions Measurement System (AEMS) and it was towed behind the vehicle. Total 46 experiments were performed on a mixed traffic route in Delhi city, and PM_{2.5} mass was collected on Teflon and quartz filter using multi-stream PM_{2.5} sampler. Total 17 trace metals (Al, Ag, As, Ba, Co, Cd, Cr, Cu, Fe, Mn, Ni, Pb, Se, Sr, Ti, V, and Zn) were characterized on Teflon filters using Induced Coupled Plasma-Mass Spectrometry (ICP-MS). Out of these metals, the non-carcinogenic and carcinogenic risks for adults and children were calculated for 5 metals namely Cr, Mn, Ni, Zn, and Pb. Trace metals concentration was highest in exhaust emitted from 4W-diesel followed by 4W-gasoline, 3W-CNG, and 2W-gasoline. Trace metals such as Cr, Mn, Ni, Zn, and Pb were present in high amount ($25.2 \pm 8.6 \mu\text{g m}^{-3}$). The carcinogenic risk from Cr was considerably higher than tolerable risk (10^{-4}), while the risk from other metals such as Ni, As, Cd, and Pb was within the range of safe (10^{-6}) and tolerable (10^{-4}) level. Overall, the human health risks associated with the exposure to PM_{2.5} emitted from gasoline and CNG vehicles were higher than that from diesel vehicle. This estimated risk in this work can help in refining the burden of disease and crafting policy to help reduce the exposures. This study is limited only for PM_{2.5} bound trace metals and associated

J. Prakash

Aerosol and Air Quality Research Laboratory, Washington University, St. Louis, MO, USA

G. Habib (✉)

Department of Civil Engineering, Indian Institute of Technology Delhi, New Delhi, India

e-mail: gazalahabib@gmail.com

© Springer Nature Singapore Pte Ltd. 2020

A. P. Singh et al. (eds.), *Advanced Combustion Techniques and Engine Technologies for the Automotive Sector*, Energy, Environment, and Sustainability,

https://doi.org/10.1007/978-981-15-0368-9_9

health risk from on-road vehicle emissions. However, poly-aromatic hydrocarbons (PAHs), perfluorinated compounds (PFCs), and semi-volatile compounds in vehicular exhaust can also impose a severe risk to human health which needs to be assessed to evaluate combined risk.

Keywords On-road vehicle · $PM_{2.5}$ · Particle-bound metals · Non-carcinogenic risk · Delhi

9.1 Introduction

On-road vehicle emissions are the significant source of air pollution especially in urban cities of India and expected rapid growth due to economic growth in India (Reynolds et al. 2011; Grieshop et al. 2012). Several toxicological studies have discussed public-health associated problems such as cardiovascular, cellular inflammation, and lung cancer risk on exposure to exhaust particle emission from on-road vehicles (Xu et al. 2013; Schwarze et al. 2013; Vreeland et al. 2016; Geller et al. 2006; Grahame et al. 2010). Recent studies have been also found that the inhalation of fine particles ($PM_{2.5}$) emitted from vehicles initiate several biochemical reactions within the body (Verma et al. 2015; Lovett 2018) leading to oxidative stress. Vehicle emission contains polycyclic aromatic hydrocarbons (PAHs), metals, carbonaceous constituents [black carbon (BC), organic carbon (OC)], inorganic acidic species (chloride, and nitrate), and complex organic compounds. However, these chemical species, especially particle-bound transition metals, have associated with oxidative stress in the human respiratory tract by reactive oxygen species (ROS) (Zhou et al. 2018; Kelly 2003; Betha and Balasubramanian 2011, 2013). Some studies have investigated particle-bound PAHs and trace metal emissions of diesel, gasoline, biodiesel vehicles using engine dynamometer in controlled laboratory conditions and during on-road operation (Betha and Balasubramanian 2011, 2013; Betha et al. 2012; Shukla et al. 2017a, b; Alves et al. 2015a). Some other studies have described the chemical composition of exhaust emission from diesel and gasoline vehicles in the European and USA fleets (Alves et al. 2015a, b). However, the particle-bound composition of European and USA fleets could be different as compared to Indian fleets, possibly due to driving conditions, road characteristics, vehicle age and category, fuel, lubricant, after-treatment technology, etc. (Jaiprakash and Habib 2017, 2018). Vehicle emission characteristics of particle-bound metals via chassis dynamometer and in tunnel experiment do not reflect the real on-road driving conditions. Therefore, in recent years, the on-road measurement directly from the tail pipe has been greatly emphasized by researchers (Wu et al. 2015, 2016). In this regard, the challenge involves in simulating the atmospheric process of gas-to-particle partitioning before collection of particle mass. Earlier studies have used a portable dilution system (PDS) and portable emission measurement system (PEMS) to carry out vehicle emission measurement under real driving conditions (Wu et al. 2015, 2016; Wang et al. 2014). However, the studies using a PDS to measure the emissions from vehicles during

on-road operation are limited (Hao et al. 2018), in addition, the characterization of particle-bound trace metals and their associated risk have not been reported in the Indian context. Therefore, this study focuses on emissions of particle-bound metals from diesel, gasoline, and CNG powered vehicles during on-road operation of mixed traffic route in Delhi city. In present work, a new Aerosol Emission Measurement System (AEMS) was used as detailed in Jaiprakash and Habib (2017). The non-carcinogenic and excess cancer risk (ECR) of particle-bound metals were estimated and presented here.

9.2 Materials and Methods

Portable dilution system (PDS) simulates the rapid cooling and dilution of exhaust as happens in the atmosphere to achieve complete gas-to-particle partitioning. The partial exhaust sample withdraws from a combustion source sampling probe and entrains into dilution tunnel, where it dilutes rapidly and homogenous with the particle and VOC free dry air (described as zero air). The dilution allows to lessen the particle number concentration inside the dilution tunnel and therefore, it avoids unwanted condensation and nucleation (Betha and Balasubramanian 2011; Betha et al. 2012; Lipsky and Robinson 2005, 2006) of the particles. In the present work, a PDS was designed following Lipsky and Robinson (2005). For on-filed measurement of any combustion sources, new PDS was subjected to reduce their compactness, incessant zero air and power supply.

9.2.1 Design of Portable Dilution System (PDS)

Figure 9.1 shows a schematic diagram of PDS, which contains 0.4 m length, and 0.1 m-diameter stainless steel dilution tunnel, 0.06 m diameter and 1.0 m length stainless duct, a heated stainless sampling probe, zero air assembly, and power supply with inverter (3 kW) and four 12 V batteries for continuous power supply for an hour. The heated sampling probe and the duct is maintained at a temperature above (~ 10 °C) the sample exhaust temperature (~ 150 °C) to avoid the thermophoresis and condensation losses (Zhang and McMurry 1992; Baron and Willeke 1993). The zero-air generation system comprised of a filter holder, an activated carbon cartridge, and molecular sieves to remove particles, volatile organic compounds, and the moisture, respectively, and the atmospheric air is stored in a reservoir (volume of 40 L) to produce continuous zero air. A dual-stage tower automatically regenerates zero air by the principle of Pressure Swing Adsorption (PSA), where the total pressure of assembly “swings” between high pressure in feed and low pressure in regeneration (Ruthven et al. 1994; Rezaei and Webley 2009). The particle sampling probe extracts a portion of the exhaust sample directly from the exhaust tailpipe by the principle of eductor technique. In eductor technique, the pressurized zero air flows at high speed

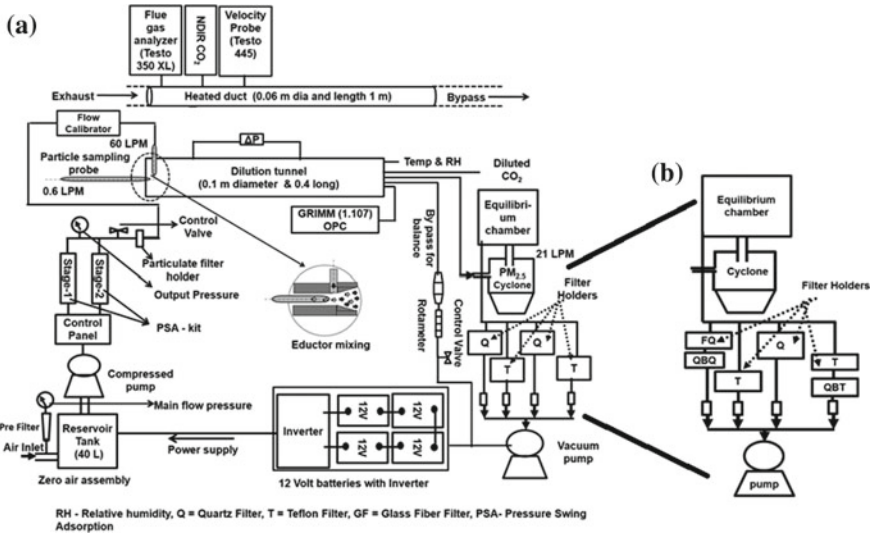


Fig. 9.1 Set-up of portable dilution sampling (PDS) system containing duct, dilution tunnel, particle sampling probe, zero air assembly, multi-stream particle sampler, and power supply unit

around the tip of the sampling probe and creates a negative pressure zone which draws the sample exhaust inside the probe without applying any control device (Harsha et al. 2019). The exhaust sample flow (~0.2–1 LPM) was induced in the sampling probe by maintaining zero air. In order to achieve the maximum dilution ratio of 100:1 (i.e. volume of zero air ÷ volume of sample exhaust) and complete aerosol formation and growth to stabilize in 3 s, the dilution tunnel of 3 L capacity was designed. The total six sampling ports were used to measuring a particle, number particle, diluted CO₂, moisture, temperature, at the downstream of dilution tunnel. One port was fixed to measure the PM_{2.5} particles using a multi-stream PM_{2.5} sampler.

9.2.2 Multi-stream Aerosol Sampler

A multi-stream PM_{2.5} sampler, which consists of an AIHL aluminium cyclone and two dual stage and two single stage filter holders (Habib et al. 2008; Venkataraman et al. 2005). The configuration details of multi-stream PM_{2.5} sampler is shown in Fig. 9.1b. This sampler provides the collection of particles with cut off aerodynamic diameter smaller than 2.5 μm at 20.2 LPM. The two filter holders were used to collect PM_{2.5} mass on a quartz filter (Pall flex 2500 QAT-UP; 47 mm, Tissue quartz) and another 2 filter holders were used to collect PM_{2.5} on Teflon membrane filters (47 mm, 2-mm pore size, Whatmann Corp., PA, USA). The flow rates of these filter holders are maintained by critical orifices (6.3, 4.5, 5.0, and 4.4 LPM) (Fig. 9.1b). In dual-stage of filter, the backup quartz filter was used to collect the artifacts, which

were determined by OC-EC analysis using Thermal optical transmittance (TOT) analyzer.

9.2.3 Evaluation of Dilution Tunnel

9.2.3.1 Gas-to-Particle Conversion

The new particle formation from gas to particle partitioning during the dilution favors the absorption of volatile organic compounds and adsorption on pre-existing inert components such as elemental carbon and minerals (sorptive material). The residence time is the time the aerosol remains in the dilution tunnel before collection, it is calculated as the ratio of the volume of dilution tunnel to total flow rate (Eq. 9.1). For dilution tunnel experiments the residence time of 2–3 s (Lipsky and Robinson 2005) and the ratio of residence time to phase equilibrium time greater than 4 are recommended to accomplish complete gas-to-particle partitioning for particles of size few 0.03–1.0 μm. The phase equilibrium time is defined as the time required by supersaturated cool vapour phase species to form new particles or to condense on existing organic particles. The residence time and phase equilibrium time scale (τ) were estimated using the following equations (Eqs. 9.1–9.4):

$$t = \frac{V_{dt}}{Q_{ex} + Q_{air}} \quad (9.1)$$

$$\tau = \frac{1}{2\pi D \sum d_p N(d_p) f_n(K_n)} \quad (9.2)$$

$$f_n(K_n) = \frac{1 + Kn}{1 + 1.71Kn + 1.33Kn^2} \quad (9.3)$$

$$Kn = \frac{2\lambda}{d_p} \quad (9.4)$$

where, V_{dt} is the volume of dilution tunnel in (m³), Q_{ex} and Q_{air} are the flow rate (m³ s⁻¹) of exhaust sample and zero air. d_p is the count median diameter of particle, N is the total number of concentration, D is the diffusion coefficient for the organic vapor in air (assumed 5×10^{-6} m² s⁻¹), $f_n(K_n)$ is the correction factor accounting for non-continuous effects, K_n is the Knudsen number, and λ is mean free path (assumed 0.065×10^{-6} m).

The phase equilibrium time for 99% condensation of volatiles was estimated by assuming heterogeneous condensation of vapor phase species in a typical particle number distribution in the dilution tunnel reported for diesel vehicles (Venkataraman et al. 2005; Matti Maricq and Maricq 2007). The size distribution was used in Eqs. (9.1)–(9.4) to determine the phase equilibrium time (τ) at different dilution ratios 40–70. The residence and phase equilibrium time at different dilution ratios

were estimated in the range of 4.3–7.5 and 0.32–0.56 s, respectively. Thus, the ratio of t/τ was calculated in the range of 8–23, which indicates that complete gas to particle partitioning can be achieved at dilution ratios between 40 and 70.

9.2.3.2 Particle Losses and Homogenous Mixing

The determination of the particle loss of PDS was evaluated using sodium chloride NaCl (NaCl ; 5 mg L^{-1}), which has polydisperse particle size range (20–600 nm). The schematic experimental set-up is shown in Fig. 9.2. The aerosol is generated from a 20 mL solution of NaCl using an aerosol generator (Model 3076, TSI Particle Instrumentation Inc., St. Paul, MN, USA) to generate 20–600 nm particle at 0.3 mL min^{-1} flow rate. NaCl generated particles withdraws in the dilution tunnel using sampling probe with 0.6 LPM by maintaining zero air flow at 18, 36, and 54 LPM, to achieve dilution ratios 30:1, 60:1, and 90:1, respectively. Afterward, a scanning mobility particle sizer (SMPS, Model 3936, TSI Inc., USA) containing differential mobility analyser (DMA, Model 3081, TSI Inc., USA), and a condensation particle counter (CPC, Model 3775, TSI Inc., USA) is used to measure the particle size distribution at upstream and downstream of dilution tunnel. The DMA gives a particle size in the range of 14–600 nm and it is scanned over the 135 s. Before the experiment, the system was operated with zero air and observed particle concentration in SMPS. Initially, the experiments were conducted with NaCl solution which is deliberated as without dilution tunnel (WODT), and then with dilution tunnel (WDT) (Fig. 9.2).

The number size distributions were recorded for WODT and WDT with three sets of experiments at the dilution ratios 30:1, 60:1, and 90:1, respectively. These particle

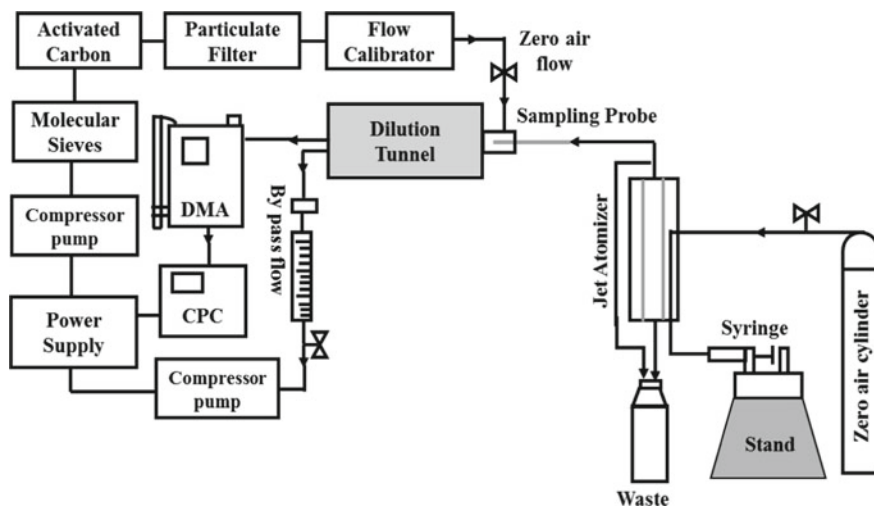


Fig. 9.2 Schematic diagram of the experimental setup used for measuring number-based particle loss in portable dilution system

size experiments are subjected to determine particle losses in the dilution tunnel. The percentage in difference between number concentration in WDT at dilution ratios and WODT were observed 6, 14, and 19%, respectively. The geometric mean diameters (GMD) were consistent 107 ± 4 , 106 ± 4 , and 104 ± 4 nm irrespective to dilution ratios implied that dilution did not affect the nucleation process. Similarly, the percentage difference between volume concentration in WDT at different dilution ratios with respect to WODT was found to be 17, 16, and 20% which shown few particle losses inside the dilution tunnel. Theoretically, thermophoresis losses were also calculated using the following equations [Eqs. (9.5)–(9.7)] (Hinds 1982):

$$\text{Thermophoretic velocity } (V_{th}) = \frac{-3\eta C_c H \nabla T}{2\rho_g T} \quad \text{for } d_p > \lambda \quad (9.5)$$

where

$$H = \left(\frac{1}{(1 + 6\lambda/d_p)} \right) \left(\frac{K_a/K_p + 4.4 \left(\frac{\lambda}{d_p} \right)}{1 + 2(K_a/K_p) + 8.8 \left(\frac{\lambda}{d_p} \right)} \right) \quad (9.6)$$

$$\text{Thermophoresis losses (\%)} = 100 * \left[1 - exp * \left(-\pi \frac{D_t L V_{th}}{Q} \right) \right] \quad (9.7)$$

where η = viscosity (PaS); C_c = slip correction factor, H = Thermophoretic coefficient; ∇T = Temperature gradient (K/m); ρ_g = gas density (kg/m^3); T = Exhaust temperature; λ = mean free path (m); d_p = particle diameter (μm); K_a = air thermal conductivity (W/m*K), assumed 0.026 (W/m*K); K_p = particle thermal conductivity (W/m*K), assumed 0.26 (W/m*K); D_t = dilution tunnel diameter (m; given 0.1 m); L = tube length (m, given = 0.4 m); Q = gas flow rate (m^3/s).

For particle mean diameter of 20, 50, and 130 nm, thermophoresis losses were estimated as <0.5% for diesel and gasoline engine. The particle and number size distribution was reported in previous studies (Gupta et al. 2010; Agarwal et al. 2015a), and adopted for calculating the thermophoresis losses.

The homogenous mixing reduces the possibility of wall losses in the dilution tunnel. To confirm homogenous mixing in dilution tunnel, PDS was performed controlled laboratory experiments using a medium duty diesel vehicle (INNOVA, BS-III, 2400 cc) on chassis dynamometer facility at Manesar Gurgaon. Only 4 experiments were planned due to high utilization rent and limited availability of chassis dynamometer. A small portion of the exhaust sample was carried from the tail-pipe using heated stainless steel (SS) sampling probe. The zero air (dilution air) flows at high pressure around the tip of sampling probe, which mixed rapidly and co-axially with exhaust sample in the dilution tunnel to attain adequate aerosol formation which occurs in the atmosphere.

For mixing, CO₂ concentrations were monitored at four ports such as 100, 200, 300 and 400 cm from the upstream of the dilution tunnel and also monitored at radial distances across the dilution tunnel. The CO₂ concentration showed insignificantly at

four ports along the distance of the dilution tunnel. The low coefficient of variances (4–10%) were observed around mean CO_2 concentration (1100 ± 60 , 800 ± 40 , 700 ± 30 , and 400 ± 40 ppm at dilution ratios 30:1, 60:1, 90:1, and 120:1, respectively) indicate rapid and homogeneous mixing inside the dilution tunnel.

To confirm particle loss, $\text{PM}_{2.5}$ particle mass were collected on quartz filters using a multi-stream aerosol sampler and examined for elemental carbon (EC) using thermal optical transmittance (TOT model DRI 2001) analyzer. The EC mass emission factors (g kg^{-1}) were consistent at different dilution ratios (30, 60, 90, and 120), which indicated insignificant particle losses in the dilution with the increase in dilution ratio. These results are discussed earlier and detailed in Jaiprakash et al. (2016). However, a declining trend in $\text{PM}_{2.5}$ emission factor was observed with increasing dilution ratio, possibly due to decreasing particulate phase OC emission and increasing gas phase OC concentration, this implied that at high dilution ratios (>70:1) the reduction in residence time (less than 2 s) limit the gas-to-particle partitioning. Therefore, the dilution ratios between 30 and 70 were found appropriate for complete gas-to-particle partitioning, and further, these dilution ratios were used for on-road experiments.

9.2.4 Aerosol Emission Measurement System

For on-road experiments, a heated duct, a portable dilution system (PDS), multi-stream $\text{PM}_{2.5}$ sampler, a gas analyzer, an exhaust velocity probe, a temperature, and relative humidity probe is mounted on Aerosol Emissions Measurement System (AEMS) behind passenger cars (Fig. 9.3). The duct was tightly fixed to the vehicle tailpipe using a stainless steel coupler with silicon gasket to avoid intrusion of

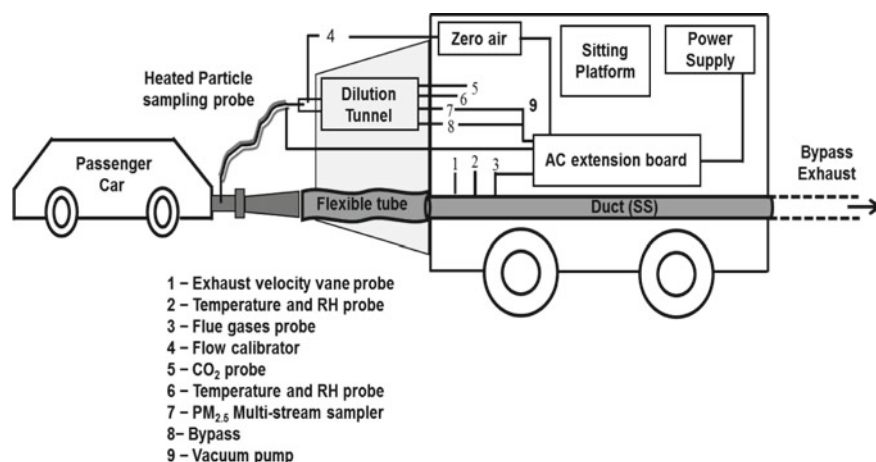


Fig. 9.3 Schematic experimental set up of aerosol emission measurement system

background air inside the duct. It should be noted that AEMS was dragged by 4-wheelers, therefore the on-road experiments were considered as under full engine load condition. In order to assess the effect of drag, three separate experiments were conducted with 4W-diesel vehicle [Bharat stage (BS)-IV 1.3 L, vehicle model post-2010] by removing the AEMS and PDS and other parts mounted in the backside of the vehicle and operate with same traffic route. The differences in PM_{2.5} emissions between without AEMS and with AEMS were 20% for the same vehicle on the same route during the same traffic hours. This difference can be attributed to the drag on emissions due to towing the AEMS behind the vehicle.

For on-road experiment, 4W-passenger (4Ws) were chosen of the different fuel type such as diesel, gasoline, and CNG and various vintage age groups (post-2000, post-2005, and post-2010) considering to Bharat Stage (BS-II, III, and IV) norms and different fuel category such as compressed natural gas (CNG) for aerosol emission measurements. All vehicles specification of tested vehicles is tabulated in Table 9.1 and discussed in the next section.

In BS-II and BS-III of diesel vehicles, the after-treatment devices were equipped with exhaust gas recirculation (EGR) which does not have any special system for conversion of NO_x and particulate matter (PM). In BS-IV, diesel vehicles engine was improved with turbocharger and after treatment device as diesel oxidation catalyst (DOC). A turbocharger is used for better air to fuel mixing for complete internal combustion and benefits to the oxidation process of DOC which oxidize CO, HC, and some of the soluble organic fraction (SOF) of diesel particulate matter but it is vain for soot particles (Dutkiewicz et al. 2009). In present study, tested Innova (post-2000, 2.4 L, BS-II), Swift Dzire (post-2012, 1.2 L, BS-IV) and Ertiga (post-2010, 1.3 L, BS-IV) diesel vehicles were equipped with common rail direct ignition (CRDI) engine, whereas Indica (post-2005, 1.4 L, BS-III) diesel vehicle equipped with direct ignition or compressed ignition (CI) (Table 9.1). For gasoline, old engines of Zen vehicle (post-2000, 1.0 L, BS-II) was equipped with spark ignition (SI) and new vehicles Swift Dzire (post-2005, 1.2 L, BS-III) and i10 (post-2005, 1.2 L, BS-IV) were found with multi-point fuel ignition (MPFI) (Table 9.1). In SI engines, the spark plug is used to adapt the combustion whereas CRDI engines are the direct injection of the fuel into the cylinders of a diesel engine from a single, common line. In gasoline-powered vehicles, the after-treatment device comprises three-way catalytic (TWC) and EGR. The function of TWC to reduce the Nitrogen Oxides (NO_x) to N₂ and O₂, and to react CO and HC, and converted into CO₂ and water (H₂O). In 3Ws-CNG, an old and new vehicle was found with SI and MPFI engines, which were equipped with carburetor and TWC as after-treatment devices. This catalyst converts all three harmful pollutants to harmless species (Haywood and Ramaswamy 1998).

Overall, nine 4W-passenger cars [4 diesel + 3 gasoline + 2 CNG, every 3 sets of the experiment] were performed for on-road experiments. Before each experiment, the vehicle engine is at rest for half an hour prior to being started [i.e. no vehicle soak time], therefore, in the present work, the emissions were considered as hot start condition only. The qualified drivers and a fixed traffic route of 10 km for ~45 min were used for on-road experiments in Delhi city. The traffic route was containing low and mixed traffic regions including 6 traffic signals. The vehicle speed was monitored

Table 9.1 Specification of tested vehicles for on-road experiments using AEMS

Vehicle model	Bharat stage norms	Year	Engine technology	After-treatment devices	Engine capacity (L)	Odometer reading (km)
Innova (N = 3)	BS-II	2004	CRDI	EGR ^a	2.4	185,032
Indica (N = 4)	BS-III	2007	CI	EGR	1.4	86,384
Swift Dzire (N = 3)	BS-IV	2012	CRDI	EGR + DOC	1.2	128,454
Ertiga (N = 6)	BS-IV	2014	CRDI	EGR + DOC	1.3	33,127
<i>4W-gasoline</i>						
Zen (N = 3)	BS-II	2001	SI	TWC + EGR	1.0	127,294
Swift Dzire (N = 3)	BS-III	2008	MPFI	TWC + EGR ^b	1.2	85,454
i10 (N = 3)	BS-IV	2010	MPFI	TWC + EGR ^c	1.2	46,550
<i>4W-CNG</i>						
Opra (N = 3)	BS-III	2006	SI	TWC + EGR	1.2	114,944
i10 (N = 3)	BS-IV	2010	MPFI	TWC + EGR ^c	1.2	46,956
<i>3W-CNG</i>						
Bajaj (N = 3)	BS-II	2008	SI	Carburetor + TWC	0.8	48,543
Bajaj (N = 3)	BS-III	2015	MPFI	Carburetor + TWC	0.8	14,817
<i>2W-gasoline</i>						
Caliber (N = 3)	BS-I	2001	SI	Carburetor	0.12	47,709
Activa (N = 3)	BS-II	2009	SI	Carburetor + TWC	0.12	28,543
Activa (N = 3)	BS-III	2014	SI	Carburetor + TWC	0.12	2973

Note N no. of the experiment; CNG compressed natural gas; BS Bharat stage; EGR exhaust gas recirculation; TC turbocharger; DOC diesel oxidation catalyst; TWC three-way catalytic converter

^aEGR with cooler for diesel vehicle

^bTWC + EGR with oxygen sensor heating capabilities for cold-start operation

^cTWC + EGR with coupler catalyst

with pocket global positioning monitor (GPS, GarminModel 60 CSx). The vehicle speed ranged between 09 and 55 km h⁻¹ with a mean speed of 25 km h⁻¹ in Delhi city.

For 2Ws-gasoline and 3Ws-CNG, experiments were carried out on a stationary position by suspending the wheels with the help of jack. With the limitations of road friction and drag, 2Ws-gasoline and 3Ws-CNG vehicles were considered to be performed under no-load condition. In the present work, the driving cycle (108 s = one cycle) was followed Modified Indian Driving Cycle (MIDC) reported in ARAI (2008) it was repeated 20 times (total 10 cycles; 1080 s = 36 min) for the collection of adequate PM_{2.5} mon the filter for chemical speciation analysis. Hence, the concentrations of 2Ws-gasoline and 3Ws-CNG were compared with earlier work and performed on engine dynamometer or stationary condition (Agarwal et al. 2015b; Aslam et al. 2006; Machacon et al. 2000).

Appropriate dilution of exhaust should be maintained during the measurement to accomplish complete gas-to-particle partitioning. In this work, the dilution ratio was calculated as the ratio of CO₂ concentration in the undiluted exhaust inside the duct and the diluted exhaust inside the dilution tunnel. The dilution ratio around 39–69 was found appropriate for complete gas-to-particle partitioning in separate experiments conducted with diesel vehicle operated on a chassis dynamometer under controlled laboratory conditions as discussed in Sect. 9.2.3.2. Significant particle losses were observed at the DRs lower than 39 and higher than 69. Therefore, during on-road experiments, the dilution ratio was maintained around DR 55 ± 11 by regulating the zero air. Out of 49 experiments 46 were finally selected based on appropriate dilution ratio, and rest three experiments were rejected due to high dilution ratio.

9.2.5 Gravimetric and Trace Metal Analysis

For gravimetric analysis, the Teflon filters were conditioned under controlled temperature (25 °C) and relative humidity (RH; 50%) for 24 h before and after the sampling. The before and after sampling, the filters were weighed using a microbalance (Sartorius, CPA2P-F). Gravimetrically PM_{2.5} concentrations were calculated by the difference between post and pre-weight of the filters and dividing by sampled exhaust volume. Six Teflon filters (3 field + 3 dynamic) were considered as blank and subjected to same pre-and post-conditioning protocol.

For trace metal analysis, half of the Teflon filter was cut into several pieces and kept in a beaker. Twenty millilitre (ml) nitric acid (70% Supra Pure, Merck GR Grade) was added into a beaker and was heated for ~2 h at 180 °C until the nitric acid gets evaporate. The remaining amount was filtered with 0.22 μm MilliPore PTFE filter and mixed Milli-Q water to make up to 100 ml and then it is subjected to further metals analysis (Gupta et al. 2011; Herlekar et al. 2012). Seventeen trace metals (Al, Ag, As, Ba, Co, Cd, Cr, Cu, Fe, Mn, Ni, Pb, Se, Sr, Ti, V, and Zn) were analyzed using Inductively Coupled Plasma–Mass Spectrometer (ICP-MS, Agilent, 7900). The trace metals mass on dynamic and field blank filters were found in the

range of 0.2–22% of the mass is determined on samples. The blank filter mass was used to correct the trace element concentration.

9.2.6 Human Health Risk Estimation

The human health risk was assessed based on average mass concentrations of trace metals from on-road experiments, which is especially useful in understanding the health hazard associated with inhalation exposure to PM_{2.5} emitted from diesel, gasoline, and CNG vehicles. During on-road emissions, the exhaust gets rapid dilution and dispersion after exiting the tail pipe. Therefore, human exposure should be calculated for ambient concentration after dilution. Similarly, in the present work, on an average 55 ± 11 times diluted particle collected on filter papers and detected metals concentrations and used for health risk estimates. Since inhalation is typically the main path to direct exposure to PM_{2.5}-bound metals. Therefore, this work examined the health risks associated with particle-bound trace metals over inhalation only.

9.2.6.1 Average Daily Dose

In the present work, the average daily dose (ADD) was estimated for particle-bound metals for inhalation route only, and following Singh and Gupta (2016). The PM_{2.5} exposure was estimated in terms of lifetime average daily dose (ADD_{inh} in mg kg⁻¹ day⁻¹). This can be expressed as follows:

$$ADD_{inh} = \frac{C \times IR \times CF \times EF \times ED}{BW \times AT_n} \quad (9.8)$$

where C is the concentration of the particle-bound metals (reported in μg m⁻³), IR is the inhalation rate, CF is a correction factor as 0.001, EF is the exposure frequency (days year⁻¹), ED is the exposure duration during lifetime (in years), BW is the body weight and AT_n is the average time (in days). All values were assumed according to the Human Health Evaluation Manual (Part A and F) (USEPA 2004, 2009), and given in Table 9.2.

9.2.6.2 Non-carcinogenic Risk

Hazard quotient (HQ) and Hazard index (HI) are used to quantitatively represent the non-carcinogenic risk from species or pollutants. The hazard quotient (HQ) can be determined by Eq. (9.9) using average daily dose (ADD_{inh} in mg kg⁻¹ day⁻¹) and reference exposure level (*RfD_{inh}*) for the inhabitants taken from USEPA (2016a).

Table 9.2 Parameters and reference value used for determining non-carcinogenic and carcinogenic risk due to inhalation

Parameter	Definition	Units	Value	
			Children	Adult
IR ^a	Inhalation rate	m ³ day ⁻¹	10	20
EF ^b	Exposure frequency	days year ⁻¹	350	350
ED ^a	Exposure duration	years	6	24
BW ^b	Body weight	kg	15	70
AT _n ^a	Average time	days	365*ED	365*ED
ET [*]	Exposure time	h day ⁻¹	10	10
Trace metals	RfD _{inh} ^c (mg kg ⁻¹ day ⁻¹)	^d IUR (μg m ⁻³) ⁻¹		
Cr(VI) [§]	2.86E-05	0.012		
Cu	4.02E-02	-		
Mn	1.43E-05	-		
Ni	3.52E-03	0.00024		
Pb	3.52E-03	0.000012		
Zn	3.01E-01	-		
As	3.0E-04	0.0043		
Cd	1.0E-03	0.0018		
V	7.0E-03	-		

^aUSEPA (2011)^bUSEPA (2013)^cUSEPA (2016b)^dUSEPA (2016b)*Exposure time is used in the present study 2 h day⁻¹[§]Cr(VI) concentration is 1/7 of total Cr

$$HQ = \frac{ADD_{inh}}{RfD_{inh}} \quad (9.9)$$

The $HQ \leq 1$ indicates no adverse health effects and $HQ > 1$ which describes likely to non-carcinogenic effects (USEPA 2016a). Hazard Index (HI) is the summation of all (HQ) estimated for different species calculated using Eq. (9.10) following Zheng et al. (2010). If the value of $HI \leq 1$, it is ideally believed that there is no non-carcinogenic risk, while $HI > 1$, it means there is a significant chance of non-carcinogenic risk.

$$HI = \sum_{i=1}^{i=n} HQ_1 + HQ_2 + HQ_3 \cdots HQ_i; \quad i = 1^{\text{st}} \text{ to } n^{\text{th}} \text{ element} \quad (9.10)$$

9.2.6.3 Carcinogenic Risk

The carcinogenic risk (in terms of Excess cancer risk; ECR) can be assessed and it is defined as the incremental probability of emerging cancer cell due to exposure of carcinogen over a lifetime. The ECR can be articulated as the following equation:

$$ECR = \frac{C \times EF \times ET \times ED \times IUR}{AT} \quad (11)$$

where C is the average concentration of particle-bound metals (in $\mu\text{g m}^{-3}$), EF is the exposure frequency (days year⁻¹), ET is the exposure time (2 h day⁻¹), ED is the exposure duration (assumed to be 24 and 6 years for adults and children), AT_n is average time [($AT_n = \text{years} \times 365 \text{ days} \times 24 \text{ h day}^{-1}$); assumed 70 and 15 years for adults and children]. Inhalation Unit Risk [IUR in ($\mu\text{g/m}^3$)⁻¹] of particle-bound metals (Table 9.2) were obtained from USEPA with the Integrated Information Risk System (<https://www.epa.gov/iris>) of USEPA.

The range of ECR has been reported by the USEPA (2009) for public health, and suggested The ECR value $< 10^{-6}$; it is ideally recommended as safe and ECR $\sim 10^{-4}$ is considered as a tolerable risk, while ECR value $> 10^{-4}$, it means there is significant high risk. In present work, the ECR was calculated only for Pb, Cr, and Ni which are well known inhaling carcinogens.

9.3 Results and Discussion

9.3.1 Trace Metals Concentration

Total 17 trace metals (Al, Ag, As, Ba, Co, Cd, Cr, Cu, Fe, Mn, Ni, Pb, Se, Sr, Ti, V, and Zn) were detected, whereas selenium (Se) was found in NAs or below detection limit (BDL) in on-road vehicles experiments, while 28 samples out of 46, Aluminium (Al) was detected as BDL. Interestingly, trace metal concentrations were highest from 4W-CNG ($76 \pm 4 \mu\text{g m}^{-3}$) followed by 3W-CNG ($62.5 \pm 15.4 \mu\text{g m}^{-3}$), 2W-gasoline ($60 \pm 21 \mu\text{g m}^{-3}$), 4W gasoline ($57 \pm 16 \mu\text{g m}^{-3}$), and were lowest from 4W-diesel ($56 \pm 8 \mu\text{g m}^{-3}$) (Fig. 9.4). It is noteworthy that the concentrations of all trace metals except Fe, Zn, Al, and Pb in present work were close to previous values ($3\text{--}10 \mu\text{g m}^{-3}$) reported in the previous work (Geller et al. 2006; Alves et al. 2015a; ARAI 2008; Schauer et al. 2002).

The major trace metals (Fe, Zn, Al, and Pb) were higher compared to previously reported values ($40\text{--}200 \mu\text{g m}^{-3}$) from diesel and biodiesel (Betha and Balasubramanian 2011, 2013). The diesel fuel and lubricant oil composition are examined by Agarwal et al. (2011) which shows diesel and lubricant oil contain high Ca, Zn, Mg, Ni and Fe in Indian fuel and it could be the possible reason which possibly due to in high concentration of these particle-bound metals in the 4Ws-diesel vehicle.

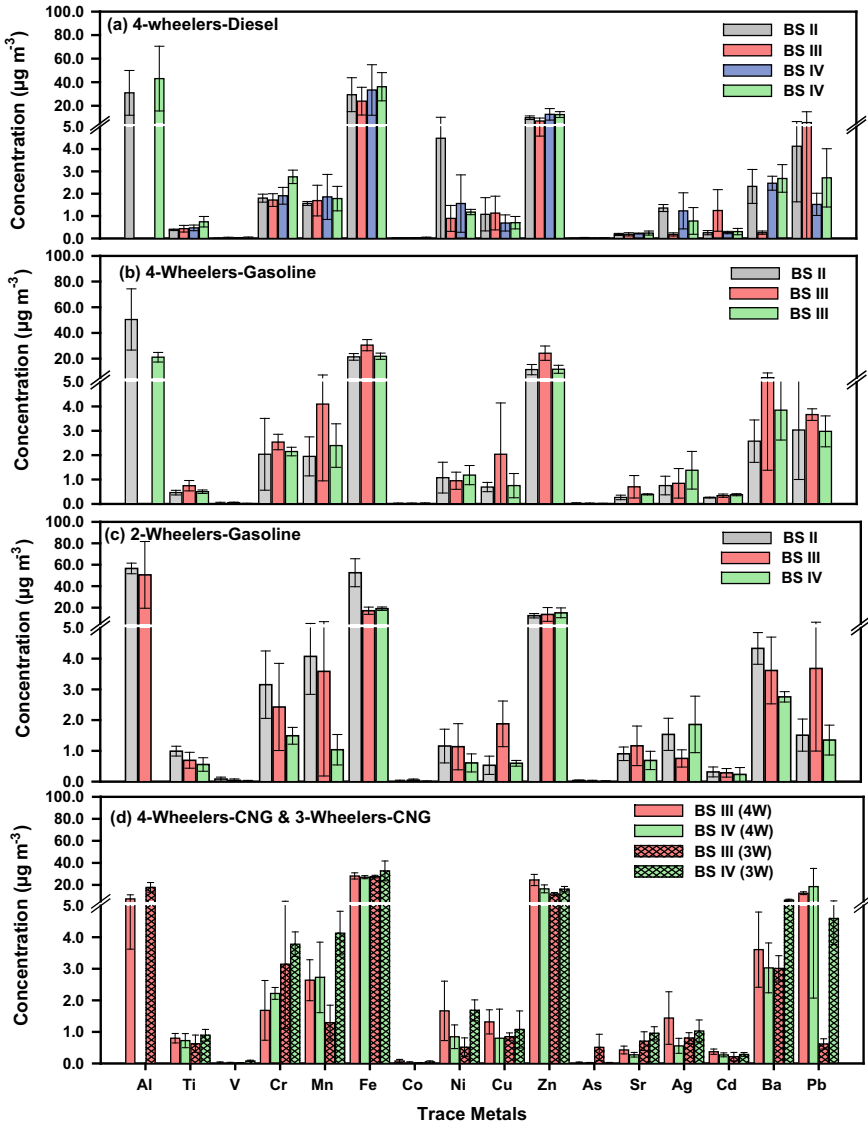


Fig. 9.4 Trace metals concentration of **a** 4-wheelers diesel; **b** 4-wheelers gasoline; **c** 2-wheelers; and **d** 4-wheelers-CNG and 3-wheelers-CNG in tail pipe exhaust

The high amount of Fe and Al can also be originated from abrasion of vehicle parts such as piston rings, valve, and cylinder liner (Agarwal et al. 2015b; Ulrich et al. 2012) and the aging of catalytic converter (Shukla et al. 2017b; Dallmann et al. 2014; Kam et al. 2012; Liati et al. 2013). The high load of zinc is mixed in lubricant oil, and antioxidant and anti-wear additive agent like Zinc-di-alkyl-di-thio phosphate (ZDDP) is used in lube oil (Alves et al. 2015a; Spikes 2004; Spencer et al. 2006). Lead (Pb) is originated in the wear of metal alloys and previous studies have been shown as contamination in diesel fuel (Dallmann et al. 2014; Chakraborty and Gupta 2010; Fabretti et al. 2009; Shukla et al. 2016). In 4Ws-diesel vehicles, the percentage of the relative contribution of trace metals were ranged 1.7–9.1%, which was higher than the range (2–5%) reported in the previous studies (Geller et al. 2006; ARAI 2009; Kam et al. 2012; Chiang et al. 2012; Kim Oanh et al. 2009; Schauer et al. 1999). Among 4Ws-gasoline vehicles, the trace metals concentrations were consistent with the age group of the vehicle (Fig. 9.4b). For 4Ws-gasoline, the concentration of trace metals was 2–4 times higher than previous studies (Geller et al. 2006; ARAI 2008; Chiang et al. 2012; Kim Oanh et al. 2009; Schauer et al. 1999) and they were contributed in the range 2.6–8.3% of $PM_{2.5}$, whereas the remaining trace metal contributions ranged between 0.5 and 2.0% of $PM_{2.5}$ and these ranges was close to percentage contribution of $PM_{2.5}$ reported in the literature. The 2Ws-gasoline showed a decrease in trend with age group of vehicles (see Fig. 9.4c). For 2Ws-gasoline, the percentage contribution of trace metals to $PM_{2.5}$ emissions was ranged between 10 and 12% and it was close to values (8–15%) examined by ARAI (2008, 2009). The percentage contribution of trace metals to $PM_{2.5}$ emissions from 3W-CNG and 4W-CNG vehicles was observed in the range of 11–13%. Again 4Ws-CNG the trace metals concentrations were consistent with age, while for 3Ws-CNG, major metals Fe, Zn, and Ba (Fig. 9.4d) varied with age.

Among trace elements, Fe and Zn have observed the highest percentage contribution to $PM_{2.5}$ in the range between 0.3 and 0.4%. Fe is mainly originated from motorised scrape of the engine and its parts (Agarwal et al. 2015a; Liati et al. 2013). The abundance of Zn is found in fuel as well as lubricant oil (Geller et al. 2006; Alves et al. 2015a; Agarwal et al. 2015a; Spencer et al. 2006). Other metals such as Cr, Cu, Fe, and Ni is also released from fuel combustion. Barium [Ba], and their oxides (barium carbonate) were also used as additives in nozzle and valves of the vehicles (Vouitsis et al. 2005). Further, Cr and Cd are also produced from engine parts (Alves et al. 2015a; Shukla et al. 2016; Gangwar et al. 2011; Gangwar et al. 2012) due to a lack of automated maintenance.

9.3.2 Human Health Risk Assessment

In the present work, 9 trace metals were considered as non-carcinogenic (As, Cd, Cr, Cu, Mn, Ni, Pb, V, and Zn) and 5 metals (As, Cd, Cr, Ni, and Pb) were considered as carcinogenic.

9.3.2.1 Average Daily Dose (ADD_{inh})

The ADD_{inh} of trace metals for adults and children is illustrated in Fig. 9.5a–e. The mean value of ADD_{inh} for adults and children showed a decreasing trend in the following order: Zn > Pb > Mn > Cr > Ni > Cu > Cd > As > V for gasoline and CNG

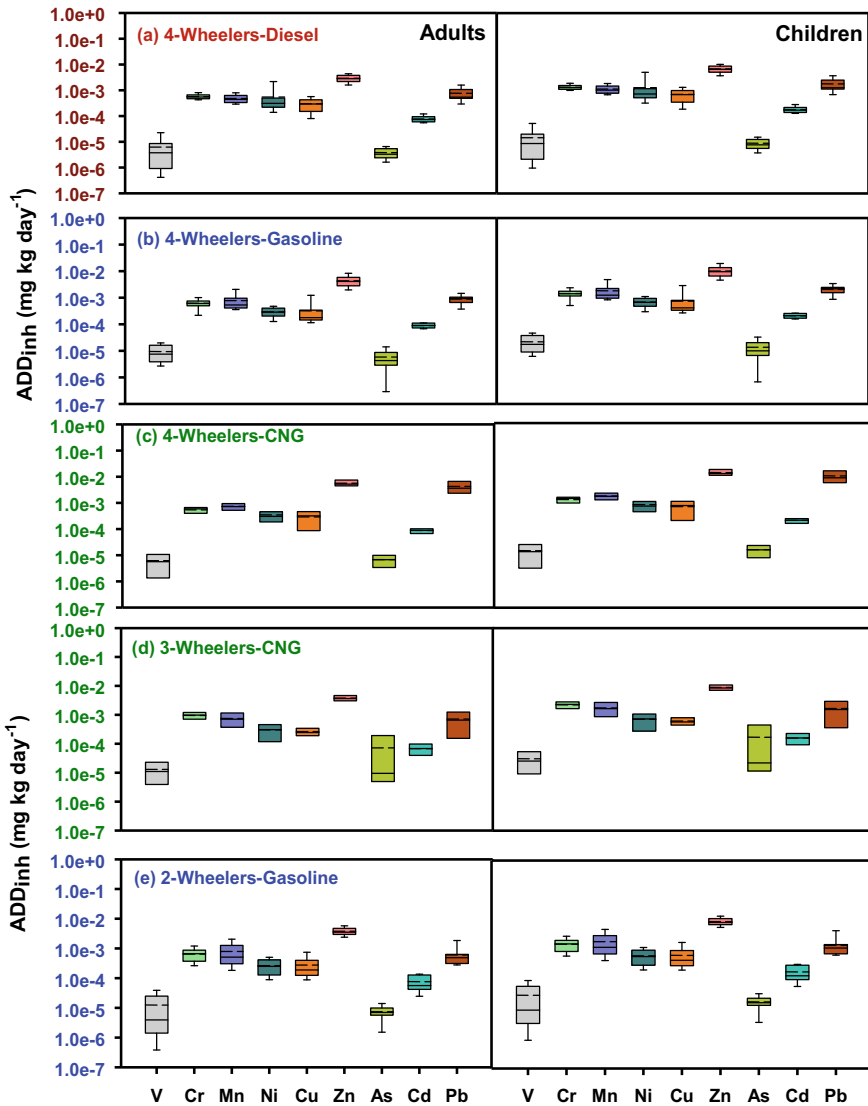


Fig. 9.5 Average daily dose (ADD_{inh}) of metals ($\text{mg kg}^{-1} \text{day}^{-1}$) on PM_{2.5} for adults (left panel) and children (right panel) from **a** 4-wheelers diesel; **b** 4-wheelers gasoline; **c** 4-wheelers-CNG 2-wheelers; **d** 3-wheelers-CNG; **e** 2-wheelers gasoline

vehicles, while the order was found as $Zn > Pb > Cr > Ni > Mn > Cu > Cd > V > As$ for diesel vehicle. The (ADD_{inh}) of Ni from 4W diesel vehicle was found to be high (~1.8 folds) as compared to (ADD_{inh}) of Ni of gasoline and CNG powered vehicles. The ADD_{inh} of Cr from gasoline and CNG vehicles were observed high (~1.6 times) as compared to diesel-powered vehicles. ADD_{inh} of Pb from 4W-CNG was observed to be 3.4 and 2.0 times higher than 3W-CNG and 2W-Gasoline vehicles. It is important to note that mean ADD_{inh} for children of metals including Cr, Mn, Ni, Cu, Zn and Pb in $PM_{2.5}$ were observed 2 times greater than mean ADD_{inh} for Adults. There was no significant difference ($p > 0.05$) observed between ADD_{inh} value of 4W Diesel and 4W-Gasoline for V, Cr, Mn, Cu, while significant difference ($p < 0.05$) in ADD_{inh} was observed for Zn and Pb emitted from 4W Diesel and 4W-CNG.

9.3.2.2 Non-carcinogenic Risk

Non-carcinogenic risk (in terms of HQs and HIs) for children and adults from on-road diesel, gasoline, and CNG vehicles were shown in Fig. 9.6a–e. The cumulative HIs from all vehicle were two times higher for children than for adults. Amongst non-carcinogenic metals, the mean level of HQ for both inhabitants (adults and children) showed in declining trend: $Mn > Cr > Ni > Pb > Cd > Zn > As > Cu > V$. For 4W-diesel vehicles, the HQ of Ni was 2 times higher than 4W-gasoline, 4W-CNG, 3W-CNG, and 2W-gasoline ($p < 0.05$) vehicles, however, other particle-bound metals such as Mn, Cr were found to be 1.6 times lower than 4W-gasoline, 4W-CNG, 3W-CNG, and 2W-gasoline vehicles. Interestingly, for adults and children, non-carcinogenic risk (HQ) was close to 1 for As, Cd, Cu, Ni, Pb, and Zn, while the HQs for Cr and Mn surpassed $HQ > 1$ (Fig. 9.6a–e) for all type of vehicles. For children, the average HI values were found in the following order: 3W-CNG > 2W-gasoline > 4W-gasoline > 4W-CNG > 4W-diesel. This indicates that possible non-carcinogenic risk due to exposure from vehicle tail pipe, abrasion of vehicle parts, which is a potential threat to inhabitants working near roads (Fig. 9.6).

This study also compared well with recent studies (Betha and Balasubramanian 2011, 2013) reported the non-carcinogenic risk of particle-bound trace metals of $PM_{2.5}$ for stationary diesel engine, biodiesel and ultra-low sulfur diesel (ULSD). Previous studies estimated HQs, and HIs using chronic daily intake (CDI), therefore present work also calculated CDI, HQs, and HIs for better comparison with previous studies. In this study, we also estimated chronic daily intake (CDI), HQs and HIs and compared with previous studies (Fig. 9.7). The present mean $\sum HQ$ was close to previously reported for ULSD engine and 36% (69 and 161 for adults and children) lower than Bio-diesel (114 and 270 for adults and children) engine for both adults and children. This shows the severity of risk from toxic metals from tail-pipe emissions in diesel, gasoline, and CNG vehicles. The composition of fuel and engine type are resulting in different level of metals emissions and their risk. It should also be noted that on-road emission and their particle bound metals could be diverse from stationary and idle tail pipe emission possibly due to the road, traffic, and driver characteristic.

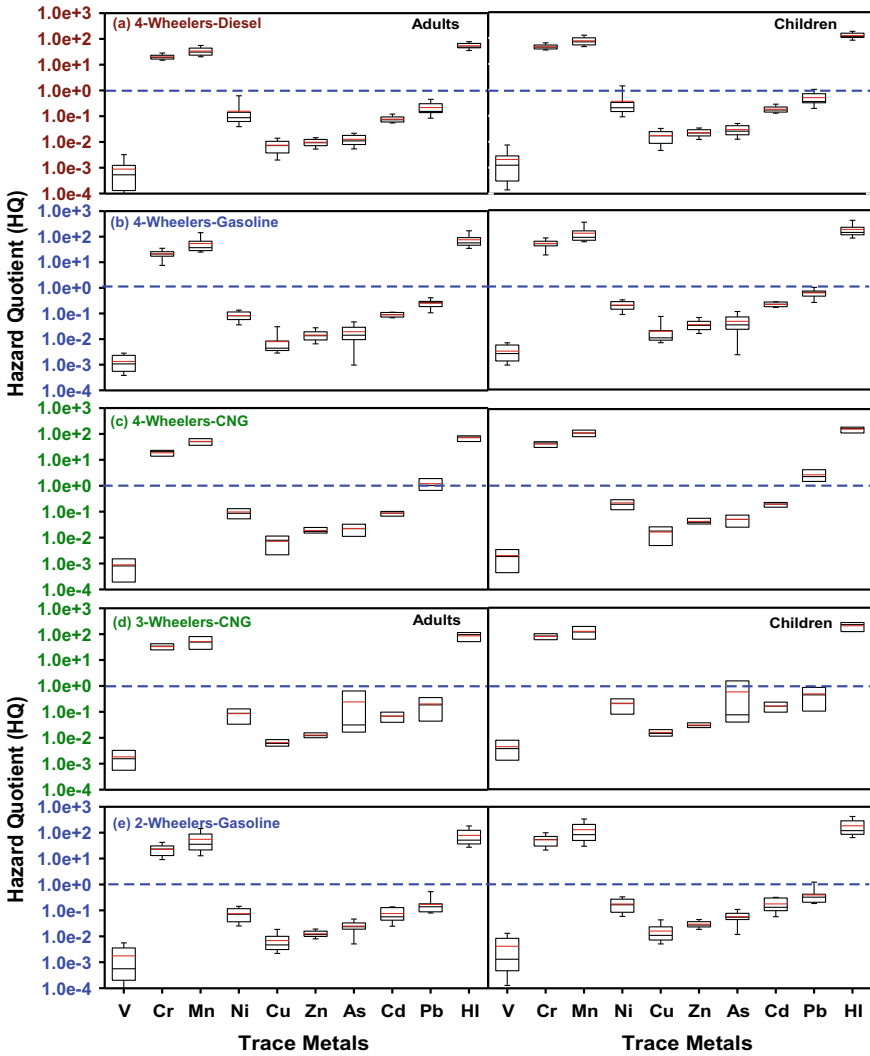


Fig. 9.6 Non-carcinogenic risks of particle-bound metals in PM_{2.5} for adults (left panel) and children (right panel) from **a** 4-wheelers diesel; **b** 4-wheelers gasoline; **c** 4-wheelers-CNG; **d** 3-wheelers-CNG; **e** 2-wheelers gasoline

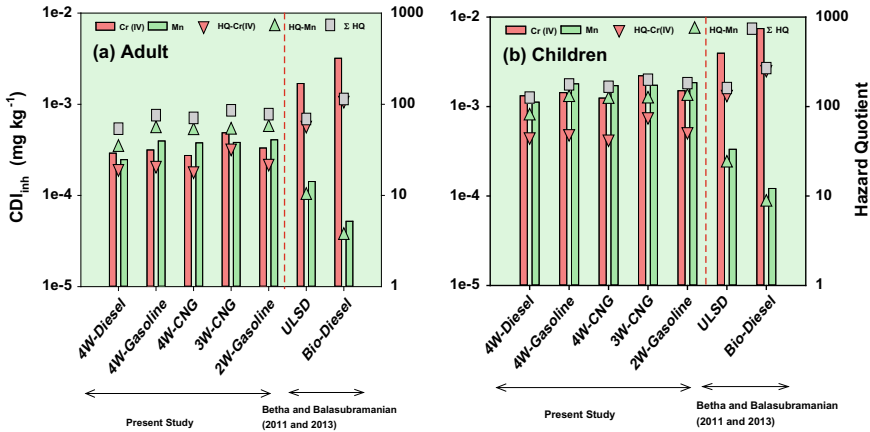


Fig. 9.7 The non-carcinogenic risk for adults (a) and children (b) in the present study and compared with previous studies (Betha and Balasubramanian 2011, 2013). Primary y-axis: bar line designates as chronic daily intake (CDI). Secondary y-axis: triangle and square represent HQs and Σ HQs for present study and previous studies. The red dotted line and arrow split the present study and previous studies

9.3.2.3 Carcinogenic Risk

In the present work, carcinogenic risk (in terms of ECR) of trace metals were estimated for the diesel, gasoline, and CNG vehicles and presented in Fig. 9.8a–e. The sum of ECR for adults was estimated as 738×10^{-6} , 794×10^{-6} , 832×10^{-6} , 696×10^{-6} , and 1239×10^{-6} for 4W-diesel, 4W-gasoline, 2W-gasoline, 4W-CNG, and 3W-CNG powered vehicles, respectively. The value of ECR for adults was showed four times higher than the value of ECR for children. The average value of ECR for Cr was showed 7–12 times higher than the acceptable limit for adults, and also 2–3 times larger than the acceptable limit for children. Significantly, the ECR value of Cr in 3Ws-CNG vehicles was estimated at 1186×10^{-6} , which was 1.5–1.8 times higher than the 4Ws-diesel and 4Ws-gasoline vehicle for both inhabitants. In 4Ws-CNG, the ECR value of Pb was marginally higher than the other vehicles. However, the mean value of ECR from Ni, As, Cd, and Pb were showed in the range of 10^{-6} – 10^{-4} for all type of vehicles (Fig. 9.8).

In the present work, the ECR from Cr for adults for diesel, gasoline, CNG vehicles are 12–24 times lower than previous work reported by Betha and Balasubramanian (2011, 2013) for ULSD and Bio-diesel engine exhaust at stationary conditions (Fig. 9.9a, b). Overall, the observed ECR values of vehicles exceed the acceptable level and suggesting that it is an alarming condition to the inhabitants of India, which works near the road. It is anticipated that the increased lung cancer mortality can arise amongst inhabitant close to road or traffic tail pipe emissions in urban cities due to inhalation of particulate-bound trace metals.

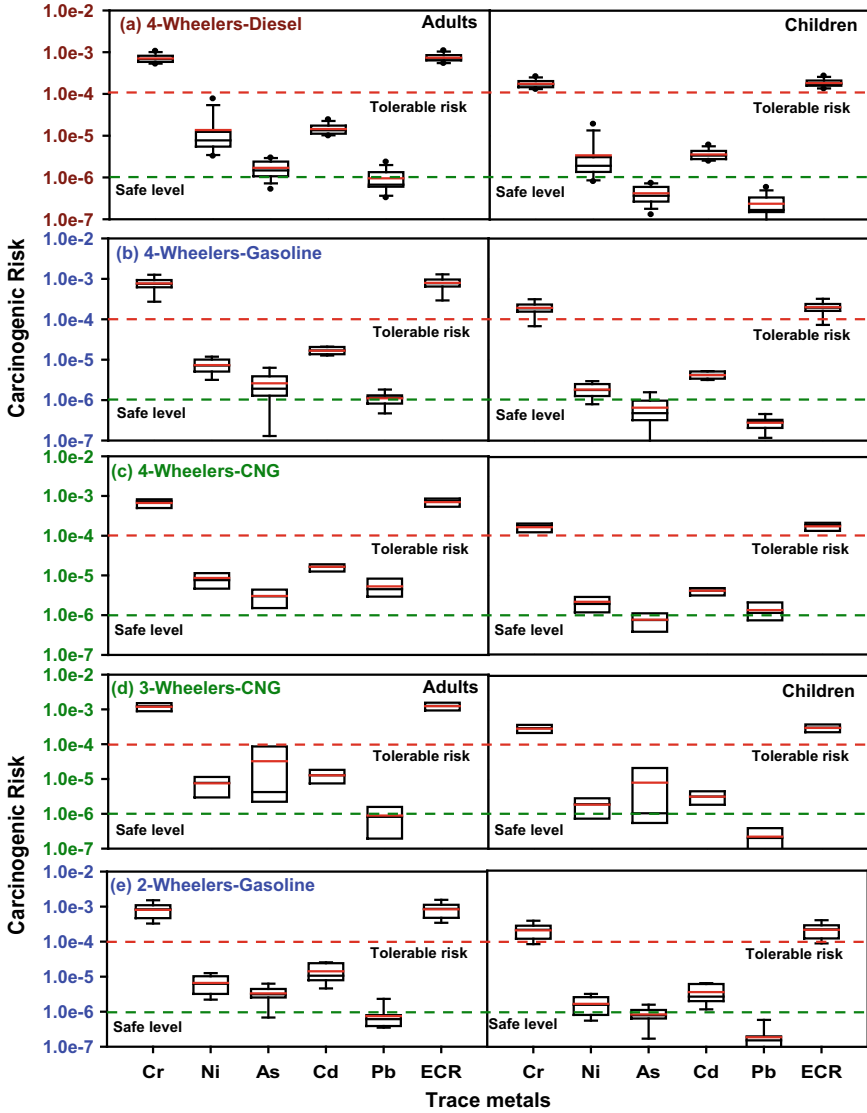


Fig. 9.8 Carcinogenic risk (as in ECR) of particle-bound metals in PM_{2.5} for adults (left panel) and children (right panel) from **a** 4-wheelers diesel; **b** 4-wheelers gasoline; **c** 4-wheelers-CNG 2-wheelers; **d** 3-wheelers-CNG; **e** 2-wheelers gasoline

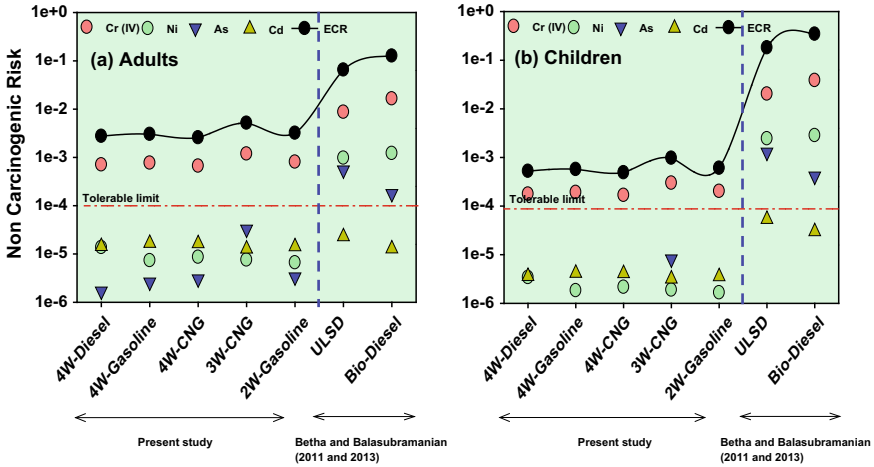


Fig. 9.9 The carcinogenic risk for adults (a) and children (b) in the present study and compared with previous studies (Betha and Balasubramanian 2011, 2013). The blue dotted line and arrow split the present study and previous studies

9.4 Conclusion

This study presents the concentration of PM_{2.5} bound trace metals emitted from the diesel, gasoline, and CNG vehicles during on-road experiments. The total trace metal emission was highest from 4W-diesel. The emissions of toxic metals such as Zn, Cr, Pb were higher from 4W-CNG and 3W-CNG vehicles compared to 4W-diesel, and 4Ws/2Ws-gasoline. The concentration of Al, Fe, Mn, Ni, As, and Cd were highest from 4W-diesel and gasoline vehicles. Health risk assessment of the PM_{2.5} bound trace metals showed that non-carcinogenic risks by Cr, and Mn, which exceeded the safe limit. The ECR of Cr was higher than the tolerance limit (10⁻⁴), while ECRs from Ni, As, Cd, and Pb was higher than the safe limits (10⁻⁶) for all types of vehicles. Additionally, it was found that the risk associated with PM emitted from 4Ws/3Ws-CNG vehicles were significantly higher compared to the risk associated with 4Ws-diesel/gasoline vehicles emissions. The present work suggests rationally robust benchmarking on emissions of PM_{2.5} bound trace metals their health risk from on-road vehicles in the Indian context. Nevertheless, the present study assessed the carcinogenic risk of particle-bound metals, but other carcinogenic compounds such as poly-aromatic hydrocarbons (PAHs) and Per-fluorinated compounds (PFCs) were not included in the risk assessment.

Acknowledgements The authors are thankful to Department of Science and Technology for supporting this work under fast track scheme (SR/FTP/ES-183/2010). We also thank Polltech Instruments Pvt Ltd, Mumbai, for valuable input in the development of PDS. We also pay a sincere gratitude to Prof. Chandra Venkataraman, IIT Bombay, and Prof. Ramya Sunder Raman, IISER

Bhopal for their support in experiments and chemical characterization work. We also thanks to students, staff and colleagues of Civil Engineering Department, IIT Delhi for their support in on-road measurement study.

References

- Agarwal AK, Gupta T, Kothari A (2011) Particulate emissions from biodiesel vs diesel fuelled compression ignition engine. *Renew Sustain Energy Rev* 15:3278–3300. <https://doi.org/10.1016/j.rser.2011.04.002>
- Agarwal AK, Gupta T, Bothra P, Shukla PC (2015a) Emission profiling of diesel and gasoline cars at a city traffic junction. *Particuology* 18:186–193. <https://doi.org/10.1016/j.partic.2014.06.008>
- Agarwal AK, Bothra P, Shukla PC (2015b) Particulate characterization of CNG fuelled public transport vehicles at traffic junctions. *Aerosol Air Qual Res* 15:2168–2174. <https://doi.org/10.4209/aaqr.2015.02.0084>
- Alves CA, Barbosa C, Rocha S, Calvo A, Nunes T, Cerqueira M, Pio C, Karanasiou A, Querol X (2015a) Elements and polycyclic aromatic hydrocarbons in exhaust particles emitted by light-duty vehicles. *Environ Sci Pollut Res* 22:11526–11542. <https://doi.org/10.1007/s11356-015-4394-x>
- Alves CA, Gomes J, Nunes T, Duarte M, Calvo A, Custódio D, Pio C, Karanasiou A, Querol X (2015b) Size-segregated particulate matter and gaseous emissions from motor vehicles in a road tunnel. *Atmos Res* 153:134–144. <https://doi.org/10.1016/j.atmosres.2014.08.002>
- ARAI (2008) Emission factor development for Indian vehicles. In: Air quality monitoring project-Indian clean air programme. The Automotive Research Association of India, Pune
- ARAI (2009) Source profiling for vehicular emissions. In: Air quality monitoring project-Indian clean air programme. The Automotive Research Association of India, Pune. http://www.cpcb.nic.in/Source_Profile_Vehicles.pdf
- Aslam MU, Masjuki HH, Kalam MA, Abdesselam H, Mahlia TMI, Amalina MA (2006) An experimental investigation of CNG as an alternative fuel for a retrofitted gasoline vehicle. *Fuel* 85:717–724. <https://doi.org/10.1016/j.fuel.2005.09.004>
- Baron PA, Willeke K (1993) Aerosol measurement: principles, techniques, and applications. Van Nostrand Reinhold, New York
- Betha R, Balasubramanian R (2011) Emissions of particulate-bound elements from stationary diesel engine: characterization and risk assessment. *Atmos Environ* 45:5273–5281. <https://doi.org/10.1016/j.atmosenv.2011.06.060>
- Betha R, Balasubramanian R (2013) Emissions of particulate-bound elements from biodiesel and ultra low sulfur diesel: size distribution and risk assessment. *Chemosphere* 90:1005–1015. <https://doi.org/10.1016/j.chemosphere.2012.07.052>
- Betha R, Balasubramanian R, Engling G (2012) Physico-chemical characteristics of particulate emissions from diesel engines fuelled with waste cooking oil derived biodiesel and ultra low sulphur diesel. *Biodiesel Feed Prod Appl*. <https://doi.org/10.5772/53476>
- Chakraborty A, Gupta T (2010) Chemical characterization and source apportionment of submicron (PM₁) aerosol in Kanpur Region, India. *Aerosol Air Qual Res* 10:433–445. <https://doi.org/10.4209/aaqr.2009.11.0071>
- Chiang HL, Lai YM, Chang SY (2012) Pollutant constituents of exhaust emitted from light-duty diesel vehicles. *Atmos Environ* 47:399–406. <https://doi.org/10.1016/j.atmosenv.2011.10.045>
- Dallmann TR, Onasch TB, Kirchstetter TW, Worton DR, Fortner EC, Herndon SC, Wood EC, Franklin JP, Worsnop DR, Goldstein AH, Harley RA (2014) Characterization of particulate matter emissions from on-road gasoline and diesel vehicles using a soot particle aerosol mass spectrometer. *Atmos Chem Phys* 14:7585–7599. <https://doi.org/10.5194/acp-14-7585-2014>

- Dutkiewicz VA, Alvi S, Ghauri BM, Choudhary MI, Husain L (2009) Black carbon aerosols in urban air in South Asia. *Atmos Environ* 43:1737–1744. <https://doi.org/10.1016/j.atmosenv.2008.12.043>
- Fabretti J-F, Sauret N, Gal J-F, Maria P-C, Schärer U (2009) Elemental characterization and source identification of PM_{2.5} using positive matrix factorization: the Malraux road tunnel, Nice, France. *Atmos Res* 94:320–329. <https://doi.org/10.1016/j.atmosres.2009.06.010>
- Gangwar J, Gupta T, Gupta S, Agarwal AK (2011) Emissions from diesel versus biodiesel fuel used in a CRDI SUV engine: PM mass and chemical composition. *Inhal Toxicol* 23:449–458. <https://doi.org/10.3109/08958378.2011.582189>
- Gangwar JN, Gupta T, Agarwal AK (2012) Composition and comparative toxicity of particulate matter emitted from a diesel and biodiesel fuelled CRDI engine. *Atmos Environ* 46:472–481. <https://doi.org/10.1016/j.atmosenv.2011.09.007>
- Geller MD, Ntziachristos L, Mamakos A, Samaras Z, Schmitz DA, Froines JR, Sioutas C (2006) Physicochemical and redox characteristics of particulate matter (PM) emitted from gasoline and diesel passenger cars. *Atmos Environ* 40:6988–7004. <https://doi.org/10.1016/j.atmosenv.2006.06.018>
- Grahame TJ, Schlesinger RB, Möhner M, Wendt A, Grahame TJ, Schlesinger RB (2010) Cardiovascular health and particulate vehicular emissions: a critical evaluation of the evidence. *Air Qual Atmos Health* 3:3–27. <https://doi.org/10.1007/s11869-009-0047-x>
- Grieshop AP, Boland D, Reynolds CCO, Gouge B, Apte JS, Rogak SN, Kandlikar M (2012) Modeling air pollutant emissions from Indian auto-rickshaws: model development and implications for fleet emission rate estimates. *Atmos Environ* 50:148–156. <https://doi.org/10.1016/j.atmosenv.2011.12.046>
- Gupta T, Jaiprakash, Dubey S (2011) Field performance evaluation of a newly developed PM_{2.5} sampler at IIT Kanpur. *Sci Total Environ* 409:3500–3507. <https://doi.org/10.1016/j.scitotenv.2011.05.020>
- Gupta T, Chakraborty A, Ujwal K (2010) Development and performance evaluation of an indigenously developed air sampler designed to collect submicron aerosol. *Ann Indian Natl Acad Eng* 7:189–193
- Habib G, Venkataraman C, Bond TC, Schauer JJ (2008) Chemical, microphysical and optical properties of primary particles from the combustion of biomass fuels. *Environ Sci Technol* 42. <https://doi.org/10.1021/es800943f>
- Hao X, Zhang X, Cao X, Shen X, Shi J, Yao Z (2018) Characterization and carcinogenic risk assessment of polycyclic aromatic and nitro-polycyclic aromatic hydrocarbons in exhaust emission from gasoline passenger cars using on-road measurements in Beijing, China. *Sci Total Environ* 645:347–355. <https://doi.org/10.1016/j.scitotenv.2018.07.113>
- Harsha S, Khakharia P, Huizinga A, Monteiro J, Vlugt JH (2019) In-situ experimental investigation on the growth of aerosols along the absorption column in post combustion carbon capture. *Int J Greenh Gas Control* 85:86–99. <https://doi.org/10.1016/j.ijggc.2019.02.012>
- Haywood JM, Ramaswamy V (1998) Global sensitivity studies of the direct radiative forcing due to anthropogenic sulfate and black carbon aerosols. *J Geophys Res Atmos* 103:6043–6058. <https://doi.org/10.1029/97JD03426>
- Herlekar M, Joseph AE, Kumar R, Gupta I (2012) Chemical speciation and source assignment of particulate (PM₁₀) phase molecular markers in Mumbai. *Aerosol Air Qual Res* 12:1247–1260. <https://doi.org/10.4209/aaqr.2011.07.0091>
- Hinds WC (1982) *Aerosol technology: properties, behavior, and measurement of airborne particles*. Wiley, New York
- Jaiprakash, Habib G (2017) Chemical and optical properties of PM_{2.5} from on-road operation of light duty vehicles in Delhi city. *Sci Total Environ* 586:900–916
- Jaiprakash, Habib G (2018) A technology-based mass emission factors of gases and aerosol precursor and spatial distribution of emissions from on-road transport sector in India. *Atmos Environ* 180:192–205. <https://doi.org/10.1016/j.atmosenv.2018.02.053>

- Jaiprakash, Habib G, Kumar S, Habib G, Kumar S, Kumar S (2016) Evaluation of portable dilution system for aerosol measurement from stationary and mobile combustion sources. *Aerosol Sci Technol* 50:717–731. <https://doi.org/10.1080/02786826.2016.1178502>
- Kam W, Liacos JW, Schauer JJ, Delfino RJ, Sioutas C (2012) On-road emission factors of PM pollutants for light-duty vehicles (LDVs) based on urban street driving conditions. *Atmos Environ* 61:378–386. <https://doi.org/10.1016/j.atmosenv.2012.07.072>
- Kelly FJ (2003) Oxidative stress: its role in air pollution and adverse health effects
- Kim Oanh NT, Thiansathit W, Bond TC, Subramanian R, Winijkul E, Paw-Armata I (2009) Compositional characterization of PM_{2.5} emitted from in-use diesel vehicles. *Atmos Environ* 44:15–22. <https://doi.org/10.1016/j.atmosenv.2009.10.005>
- Liati A, Schreiber D, Dimopoulos Eggenschwiler P, Arroyo Rojas Dasilva Y (2013) Metal particle emissions in the exhaust stream of diesel engines: an electron microscope study. *Environ Sci Technol* 47:14495–14501. <https://doi.org/10.1021/es403121y>
- Lipsky EM, Robinson AL (2005) Design and evaluation of a portable dilution sampling system for measuring fine particle emissions. *Aerosol Sci Technol* 39:542–553. <https://doi.org/10.1080/027868291004850>
- Lipsky EM, Robinson AL (2006) Effects of dilution on fine particle mass and partitioning of semivolatile organics in diesel exhaust and wood smoke. *Environ Sci Technol* 40:155–162. <https://doi.org/10.1021/es050319p>
- Lovett CD (2018) Toxicity of urban particulate matter: long-term health risks, influences of surrounding geography, and diurnal variation in chemical composition and the cellular oxidative stress response. Faculty of the Graduate School
- Machacon HTCC, Yamagata T, Sekita H, Uchiyama K, Shiga S, Karasawa T, Nakamura H (2000) CNG operation of a two-stroke, two-cylinder marine S.I. engine and its characteristics of self-ignition combustion. *JSAE Rev* 21:567–572. [https://doi.org/10.1016/s0389-4304\(00\)00078-3](https://doi.org/10.1016/s0389-4304(00)00078-3)
- Matti Maricq M, Maricq MM (2007) Chemical characterization of particulate emissions from diesel engines: a review. *J Aerosol Sci* 38:1079–1118. <https://doi.org/10.1016/j.jaerosci.2007.08.001>
- Reynolds CCO, Grieshop AP, Kandlikar M (2011) Climate and health-relevant emissions from in-use Indian three-wheelers fueled by natural gas and gasoline. *Environ Sci Technol* 45:2406–2412. <https://doi.org/10.1021/es102430p>
- Rezaei F, Webley P (2009) Optimum structured adsorbents for gas separation processes. *Chem Eng Sci* 64:5182–5191. <https://doi.org/10.1016/j.ces.2009.08.029>
- Ruthven DM, Farooq S, Knaebe KS (1994) Pressure swing adsorption. VCH Publishers, New York
- Schauer JJ, Kleeman MJ, Cass GR, Simoneit BRT (1999) Measurement of emissions from air pollution sources. 2. C₁ through C₃₀ organic compounds from medium duty diesel trucks. *Environ Sci Technol* 33:1578–1587. <https://doi.org/10.1021/es980081n>
- Schauer JJ, Kleeman MJ, Cass GR, Simoneit BRT (2002) Measurement of emissions from air pollution sources. 5. C₁–C₃₂ organic compounds from gasoline-powered motor vehicles. *Environ Sci Technol* 36:1169–1180. <https://doi.org/10.1021/es0108077>
- Schwarze PE, Totlandsdal AI, Låg M, Refsnes M, Holme JA, Øvrevik J (2013) Inflammation-related effects of diesel engine exhaust particles: studies on lung cells in vitro. *Biomed Res Int* 2013:1–13. <https://doi.org/10.1155/2013/685142>
- Shukla PC, Gupta T, Labhsetwar NK, Agarwal AK (2016) Development of low cost mixed metal oxide based diesel oxidation catalysts and their comparative performance evaluation. *RSC Adv* 6:55884–55893. <https://doi.org/10.1039/C6RA06021H>
- Shukla PC, Gupta T, Labhsetwar NK, Khobaragade R, Gupta NK, Agarwal AK (2017a) Effectiveness of non-noble metal based diesel oxidation catalysts on particle number emissions from diesel and biodiesel exhaust. *Sci Total Environ* 574:1512–1520. <https://doi.org/10.1016/j.scitotenv.2016.08.155>
- Shukla PC, Gupta T, Labhsetwar NK, Agarwal AK (2017b) Trace metals and ions in particulates emitted by biodiesel fuelled engine. *Fuel* 188:603–609. <https://doi.org/10.1016/j.fuel.2016.10.059>

- Singh DK, Gupta T (2016) Source apportionment and risk assessment of PM₁ bound trace metals collected during foggy and non-foggy episodes at a representative site in the indo-gangetic plain. *Sci Total Environ* 550:80–94. <https://doi.org/10.1016/j.scitotenv.2016.01.037>
- Spencer MT, Shields LG, Sodeman DA, Toner SM, Prather KA (2006) Comparison of oil and fuel particle chemical signatures with particle emissions from heavy and light duty vehicles. *Atmos Environ* 40:5224–5235. <https://doi.org/10.1016/j.atmosenv.2006.04.011>
- Spikes H (2004) The history and mechanisms of ZDDP. *Tribol Lett* 17:469–489. <https://doi.org/10.1023/B:TRIL.0000044495.26882.b5>
- Ulrich A, Wichser A, Hess A, Heeb N, Emmenegger L, Czerwinski J, Kasper M, Mooney J, Mayer A (2012) Particle and metal emissions of diesel and gasoline engines—are particle filters appropriate measures. In: 16th conference on combustion generated nanoparticles, Zürich, Switzerland, p 13
- USEPA (2004) Risk assessment: guidance for superfund volume I: human health evaluation manual (part E, supplemental guidance for dermal risk assessment) final
- USEPA (2009) Risk assessment guidance for superfund (RAGS): part F
- USEPA (2011) Human health risk assessment
- USEPA (2013) Regional screening levels (RSLs)—user’s guide
- USEPA (2016a) Regional screening levels (RSLs)—user’s guide
- USEPA (2016b) Regional screening levels (RSLs)—equations
- Venkataraman C, Habib G, Eiguren-Fernandez A, Miguel AH, Friedlander SK (2005) Residential biofuels in South Asia: carbonaceous aerosol emissions and climate impacts. *Science* 307:1454–1456. <https://doi.org/10.1126/science.1104359>
- Verma V, Fang T, Xu L, Peltier RE, Russell AG, Ng NL, Weber RJ (2015) Organic aerosols associated with the generation of reactive oxygen species (ROS) by water-soluble PM_{2.5}. *Environ Sci Technol* 49:4646–4656. <https://doi.org/10.1021/es505577w>
- Vouitsis E, Ntziachristos L, Samaras Z (2005) Modelling of diesel exhaust aerosol during laboratory sampling. *Atmos Environ* 39:1335–1345. <https://doi.org/10.1016/j.atmosenv.2004.11.011>
- Vreeland H, Schauer JJ, Russell AG, Marshall JD, Fushimi A, Jain G, Sethuraman K, Verma V, Tripathi SN, Bergin MH (2016) Chemical characterization and toxicity of particulate matter emissions from roadside trash combustion in urban India. *Atmos Environ* 147:22–30. <https://doi.org/10.1016/j.atmosenv.2016.09.041>
- Wang Z, Wu Y, Zhou Y, Li Z, Wang Y, Zhang S, Hao J (2014) Real-world emissions of gasoline passenger cars in Macao and their correlation with driving conditions. *Int J Environ Sci Technol* 11:1135–1146. <https://doi.org/10.1007/s13762-013-0276-2>
- Wu B, Shen X, Cao X, Zhang W, Wu H, Yao Z (2015) Carbonaceous composition of PM_{2.5} emitted from on-road China III diesel trucks in Beijing, China. *Atmos Environ* 116:216–224. <https://doi.org/10.1016/j.atmosenv.2015.06.039>
- Wu B, Shen X, Cao X, Yao Z, Wu Y (2016) Characterization of the chemical composition of PM_{2.5} emitted from on-road China III and China IV diesel trucks in Beijing, China. *Sci Total Environ* 551–552:579–589. <https://doi.org/10.1016/j.scitotenv.2016.02.048>
- Xu Y, Barregard L, Nielsen J, Gudmundsson A, Wierzbicka A, Axmon A, Jönsson BAG, Kåredal M, Albin M (2013) Effects of diesel exposure on lung function and inflammation biomarkers from airway and peripheral blood of healthy volunteers in a chamber study. *Part Fibre Toxicol* 10:1–9. <https://doi.org/10.1186/1743-8977-10-60>
- Zhang X, McMurry PH (1992) Evaporative losses of fine particulate nitrates during sampling. *Atmos Environ Part A Gen Top* 26:3305–3312. [https://doi.org/10.1016/0960-1686\(92\)90347-n](https://doi.org/10.1016/0960-1686(92)90347-n)
- Zheng N, Liu J, Wang Q, Liang Z (2010) Health risk assessment of heavy metal exposure to street dust in the zinc smelting district, Northeast of China. *Sci Total Environ* 408:726–733. <https://doi.org/10.1016/j.scitotenv.2009.10.075>
- Zhou J, Zotter P, Bruns EA, Stefanelli G, Bhattu D, Brown S, Bertrand A, Marchand N, Lamkad-dam H, Slowik JG, Prévôt ASH, Baltensperger U, Nussbaumer T, El-Haddad I, Dommen J (2018) Particle-bound reactive oxygen species (PB-ROS) emissions and formation pathways in residential wood smoke under different combustion and aging conditions. *Atmos Chem Phys* 18:6985–7000. <https://doi.org/10.5194/acp-18-6985-2018>